Journal of Power Sources 195 (2010) 7991–7999

Contents lists available at ScienceDirect

Journal of Power Sources

journal homepage: www.elsevier.com/locate/jpowsour

Enhanced performance of a direct methanol alkaline fuel cell (DMAFC) using a polyvinyl alcohol/fumed silica/KOH electrolyte

Shingjiang Jessie Lue[a,*], Wei-Ting Wang[a], K.P.O. Mahesh[a], Chun-Chen Yang[b]

[a] Department of Chemical and Materials Engineering, Chang Gung University, Kwei-shan, 259 Wen-Hua First Road, Taoyuan 333, Taiwan
[b] Department of Chemical Engineering, Mingchi University of Technology, Tai-shan, Taipei Hsien 243, Taiwan

ARTICLE INFO

Article history:
Received 30 April 2010
Received in revised form 14 June 2010
Accepted 15 June 2010
Available online 23 June 2010

Keywords:
Direct methanol alkaline fuel cell (DMAFC)
Cell performance
Methanol permeability
Conductivity
Membrane electrode assembly (MEA)

ABSTRACT

A novel polymer–inorganic composite electrolyte for direct methanol alkaline fuel cells (DMAFCs) is prepared by physically blending fumed silica (FS) with polyvinyl alcohol (PVA) to suppress the methanol permeability of the resulting nano-composites. Methanol permeability is suppressed in the PVA/FS composite when comparing with the pristine PVA membrane. The PVA membrane and the PVA/FS composite are immersed in KOH solutions to prepare the hydroxide-conducting electrolytes. The ionic conductivity, cell voltage and power density are studied as a function of temperature, FS content, KOH concentration and methanol concentration. The PVA/FS/KOH electrolyte exhibits higher ionic conductivity and higher peak power density than the PVA/KOH electrolyte. In addition, the concentration of KOH in the PVA/FS/KOH electrolytes plays a major role in achieving higher ionic conductivity and improves fuel cell performance. An open-circuit voltage of 1.0 V and a maximum power density of 39 mW cm^{-2} are achieved using the PVA/(20%)FS/KOH electrolyte at 60 °C with 2 M methanol and 6 M KOH as the anode fuel feed and with humidified oxygen at the cathode. The resulting maximum power density is higher than the literature data reported for DMAFCs prepared with hydroxide-conducting electrolytes and anion-exchange membranes. The long-term cell performance is sustained during a 100-h continuous operation.

1. Introduction

Fuel cells convert chemical energy into electrical energy and provide an attractive alternative power source as crude oil prices surge. Among the various types of fuel cells, the direct methanol fuel cell (DMFC) has the advantages of high energy density, low emission of pollutants, and the ability to use liquid fuel that can be easier to store and transport than hydrogen [1,2]. DMFCs are especially suitable for use in portable electronic equipments, such as laptop computers, two-way radios, mobile phones, personal digital assistants (PDA), and other devices [3,4].

The use of proton-exchange membranes (e.g., Nafion membranes) however, suffers from the cross-over of methanol through the membrane and from a requirement for large amounts of the precious platinum catalyst to achieve a high power density [5–9]. Many researchers have proposed the use of hydroxide-conducting polymer electrolytes for direct methanol alkaline fuel cells (DMAFCs) [10–14]. In the anode of a DMAFC, methanol is oxidized to carbon dioxide and water by reacting with hydroxide ions (Fig. 1(a)). Humidified oxygen or air enters the cathode and is reduced to hydroxide ions. The hydroxide ions are then transferred from the cathode to the anode, and water molecules are formed at the anode. This behavior is different from a proton-exchange DMFC, in which protons diffuse from the anode to the cathode and water is produced at the cathode. A benefit of DMAFCs is better performance of the cathode, which does not need a noble metal catalyst (such as Pt) and which permits use of a cheaper catalyst (e.g., nickel or silver) [15]. The methanol oxidation rate is faster in an alkaline media than in an acidic solution [16–19]. In addition, the OH^- anion transport direction opposes that of the methanol flux through the membrane and leads to an intrinsic reduction in methanol permeability.

Although DMAFCs can be fabricated using alkali solutions as electrolytes [20], these cells usually suffer from solution leakage and corrosion [21,22]. Anion-exchange membranes (AEMs) containing quaternary amine functional groups may be a better choice because of their capability to selectively transport hydroxide ions [5,23–25]. Kim et al. [26], Coutanceau et al. [27], Yu et al. [28], Varcoe et al. [29] and Matsuoka et al. [30] have reported on the performance of DMAFCs. Although their power densities were higher than those for DMAFCs with a Na^+-type Nafion membrane (which had a peak power density of 4.4 mW cm^{-2} at 60 °C), these results were still not satisfactory. For example, most researchers

* Corresponding author. Tel.: +886 3 2118800x5489; fax: +866 3 2118700.
E-mail address: jessie@mail.cgu.edu.tw (S.J. Lue).

0378-7753/$ – see front matter © 2010 Elsevier B.V. All rights reserved.
doi:10.1016/j.jpowsour.2010.06.049

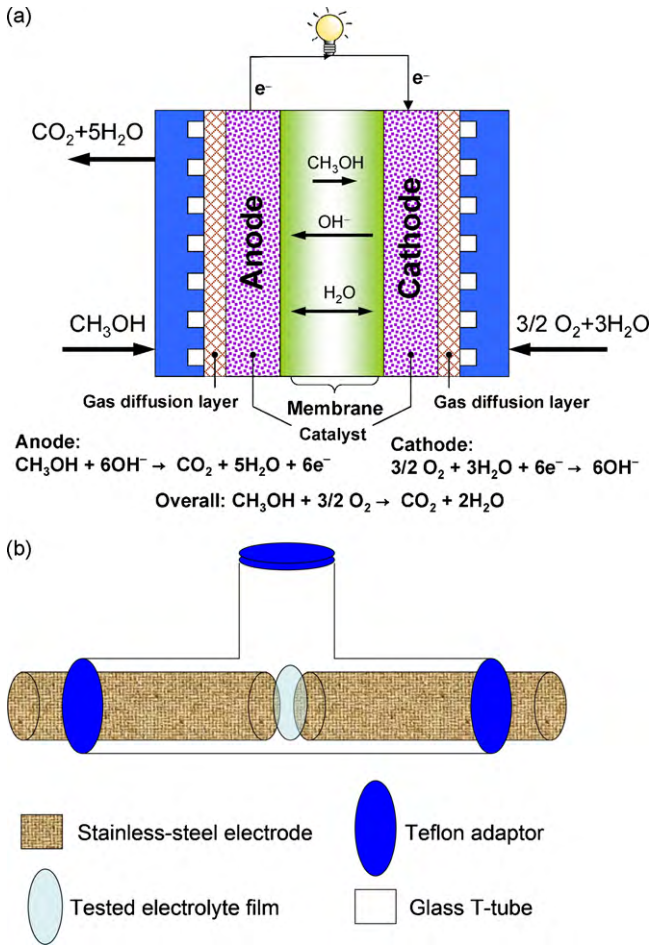

Fig. 1. Schematics of (a) experimental set-up and electrode reactions in a direct methanol alkaline fuel cell (DMAFC), and (b) electrolyte holder for conductivity measurement.

obtained power densities of less than 10 mW cm^{-2} [5,11,26,29,31]. Higher results were obtained by Yu and Scott [31] (maximum power density of 17.8 mW cm^{-2} at 60 °C) and Coutanceau et al. [27] (18 mW cm^{-2} at room temperature).

Solid electrolytes based on polymer and inorganic composites are effective alternatives as the hydroxide-conducting electrolytes. Hou et al. [32] prepared a KOH-doped polybenzimidazole (PBI) membrane electrolyte for DMAFCs and reported that the peak power density was about 31 mW cm^{-2} at 90 °C while feeding the anode with a solution containing 2 M methanol and 2 M KOH. Yang [13,33] synthesized a cross-linked polyvinyl alcohol (PVA)/TiO_2 composite for a DMAFC. The maximum power density of their DMAFC was about 7.54 mW cm^{-2} at 60 °C using a Pt/Ru black catalyst for the anode and MnO_2 carbon inks for the cathode. They also developed a PVA/hydroxyapatite (HAP) composite and achieved a peak power density of 11.48 mW cm^{-2} at room temperature [34].

In our previous work, we reported that the incorporation of fumed silica (FS) nanoparticles into a PVA matrix enhanced the thermal and mechanical properties of the resulting composites. The decomposition temperature of the PVA/FS composites was increased by adding FS [35]. The composite polymer membranes exhibited higher stability than the pristine PVA in aqueous solution. The dissolution in water was suppressed, and the crystallinity of the moistened film was maintained because of nanoparticles that acted as physical cross-linkers and inhibited PVA chain-unfolding [35]. In addition, more crystalline regions in the polymer matrix were transformed into the amorphous domain [36] with higher FS loading. The free volume was increased, and water transfer was facilitated in the PVA/FS composite [36]. Although less water was adsorbed in the PVA/FS composite, a greater percentage of water was present in the bound state [37]. This bound water does not easily evaporate, may help to maintain the ionic conductivity, and provides micro-channels for OH^- transport.

In the present work, we employed this composite as a polymer electrolyte in DMAFCs. The PVA membrane and PVA/FS composite were immersed in a KOH solution of varying concentration to provide hydroxide conductivity. The methanol transport of the PVA membrane and the PVA/FS composite was investigated. The ionic conductivities of the PVA/KOH and PVA/FS/KOH electrolytes were examined. The cell performance of the DMAFCs with these electrolytes was systematically reported as functions of FS loading level, temperature, KOH and methanol concentrations.

2. Experimental

2.1. Materials

PVA (average molecular weight of 89,000–98,000, more than 99% hydrolyzed), methanol and KOH were purchased from Sigma–Aldrich (St. Louis, MO, USA). Fumed silica (FS) with a primary particle size of 14 nm was obtained from Cabot Corp. (Carb-O-Sil M5, Tuscola, IL, USA). The materials were used as received. Pure water of 18 MΩ cm resistivity was produced using a Millipore water purifier (Elix 5/Milli-Q Gradient system, Millipore Corp., Bedford, MA, USA).

2.2. Membrane and electrolyte preparation

PVA (15 g) was dissolved in 135 g of DI water. A predetermined amount (0–3.75 g) of FS was added to the PVA polymer solution. The mixture was heated to 90 °C and continuously agitated for 6 h. The slurry was degassed in a heated ultrasonic bath for 15 min. The viscous polymer slurry was then cast onto a glass plate using an applicator knife (Model No. 3580, Elcometer Instruments Ltd., Edge Lane, England). The cast film was dried at ambient temperature for 1 day, and it was then dried in a vacuum oven at 60 °C for 8 h. The PVA membrane and PVA/FS (which contained 20% FS in most cases) composite film were peeled from the glass plate and stored in a desiccator. The thickness of the resulting membrane was 180 ± 20 mm and was measured using a digital meter (Model 345, Elcometer Instruments Ltd., Edge Lane, England). The membranes were denoted as PVA or PVA/FS. These membranes were immersed in KOH solutions (1–6 M, equal to concentrations employed in the cell performance measurements) for 10–20 min. These KOH-doped PVA and PVA/FS polymer electrolytes were denoted as PVA/KOH or PVA/FS/KOH, respectively.

2.3. Methanol permeability

Methanol permeability measurements were carried out for PVA membrane and PVA/FS composites at different temperatures using a hand-made, double-jacked, glass permeation cell. The glass cell was divided into two compartments. One reservoir was filled with 1 M methanol (aqueous), and the other receiving reservoir was filled with deionized water. The membrane was placed between these two compartments to measure the permeability of methanol. The methanol concentration transported through the membranes into the receiving reservoir was determined at regular time intervals using a gas chromatograph (HP 4890A, Agilent Technologies Co. Ltd., St. Louis, MO, USA). The experimental set-up and calcu-

lation of the methanol permeability were shown in our previous publication [38].

2.4. Ionic conductivity measurements

Conductivity measurements were made for the PVA/KOH and PVA/FS/KOH electrolytes using an alternating current (AC) impedance method. The electrolytes were sandwiched in a spring-loaded glass holder between two stainless steel electrodes with a surface area of 1.33 cm^2 each, as shown in Fig. 1(b). A thermocouple was kept in close contact with the tested electrolyte for temperature measurements. Each sample was equilibrated in KOH solution at the tested temperature for at least 30 min prior to analysis. The electrolyte holder would maintain the moisture inside the membrane and in the holder during the conductivity measurement. The AC impedance measurements were carried out using an Autolab PGSTAT-30ZN potentiostat (Eco Chemie B.V., Utrecht, The Netherlands). The resistance was recorded at AC frequencies from 10 kHz to 100 Hz at an excitation signal of 10 mV. The resistance (R_b) of the composite was calculated from the impedance data and derived from the intercept on the real axis of the Nyquist plot [38–41]. The conductivity (σ) was calculated with the $L/(R_bA)$ relation, where L is the composite thickness (cm) and A is the area of the blocking electrode (cm^2). The electrolyte conductivity was determined at various temperatures, ranging from 30 to 60 °C. The temperatures were maintained within ±0.2 °C by a conventional oven (DO45, Deng Yng, Tainan , Taiwan).

2.5. Cell performance measurements

The PVA/KOH or PVA/FS/KOH electrolyte was sandwiched between the sheets of the gas diffusion electrodes (E-tek, 5 mg cm^{-2} Pt–Ru for the anode and 5 mg cm^{-2} Pt for the cathode) to obtain a membrane electrode assembly (MEA). The area of the MEA electrode was 5 cm^2. Two flow-field plates made of high-density carbon with carved flow paths (1 mm wide and 1 mm deep) were fixed next to the MEA. Two gold-plated copper end plates were used as current collector and were assembled next to the flow-field plates. Two heating tapes were adhered to the surfaces of the end plates. A thermocouple was inserted into the end plates and the measured temperature was fed back to a controller to ensure that the cell temperature was at the set point. The experimental set-up was shown in a separate paper [42]. The thermostated methanol/KOH solution was fed into the anode at a flow rate of 5 mL min^{-1}, and humidified oxygen gas was fed into the cathode. To maintain the same fuel/oxygen stoichiometric ratio, the humidified oxygen flow rate was set at 50 or 100 mL min^{-1}, respectively, for 1 or 2 M methanol concentration. The electrochemical measurements of the DMAFCs were recorded using a constant current density mode with an electrical load (Kikusui, PLZ164WA electrochemical system, Tokyo, Japan). The cell performance of the DMAFCs was investigated as a function of methanol concentration, KOH concentration, FS loading, and temperature. The experimental errors for the open-circuit voltage and maximum power density were calculated on replicated runs at 40 °C. Long-term cell performance was recorded using a similar experimental set-up, but these experiments recycled the used methanol/KOH solution. To prevent methanol vaporization loss during the test, a lower temperature of 40 °C and 1 M methanol concentration were employed in the durability test. The cell potential was recorded at a current density of 20 mA cm^{-2} every 20 h, with a 30-min off-period. In this way, the cell potential (during the operational period) and the open-circuit potential (during the off period) could be monitored continuously for 100 h.

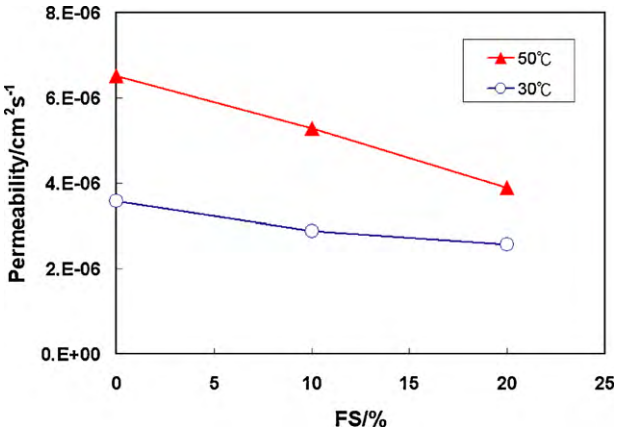

Fig. 2. Methanol permeability in PVA membranes and PVA/FS composites with different concentrations of FS in 1 M methanol at 30 and 50 °C.

3. Results and discussion

3.1. Methanol permeability

Fig. 2 shows the methanol permeability for the PVA membrane and PVA/FS composites using a 1 M methanol solution at 30 and 50 °C. The methanol permeability values of the pristine PVA membrane were 3.57×10^{-6} and 6.63×10^{-6} cm^2 s^{-1} at 30 and 50 °C, respectively. As the FS loading level was increased, the methanol permeability was reduced. For the PVA/(20%)FS composite, the methanol permeabilities were 2.58×10^{-6} and 3.88×10^{-6} cm^2 s^{-1} at 30 and 50 °C, respectively. The tortuous path in the composite structure was formed by the FS filler blending into the PVA and this resulted in an increased resistance to methanol transport. Liu et al. [43] studied the pervaporation of methanol/water mixture using PVA and poly(acrylic acid-*co*-acrylnitrile)/SiO_2 composites. They found that the selectivity of water over methanol was increased with FS addition and the FS-containing composites made the permeation easier for water and more difficult for methanol molecules. When the temperature was raised, the methanol permeability increased for all of the PVA and the PVA/FS composites because the methanol diffusion rate is greater at a higher temperature.

Yang et al. [44] reported that the methanol permeability of PVA/20% montmorillonite (MMT) composites was 2.85×10^{-6} cm^2 s^{-1} at 25 °C, which was about 10% higher than that of the PVA/(20%)FS composite in this study. These PVA/FS composites containing the FS nanoparticles (with a particle size of 14 nm) may lead to the formation of more free volume when compared with the MMT ceramic filler (with a particle size of 6–16 μm) in the PVA matrix. The nanoparticles provided a higher number of particles per unit mass than the micron-sized fillers; therefore, the methanol permeability of the PVA/FS composite was lower than that of the PVA/MMT composite.

3.2. Ionic conductivity

The resistance and ionic conductivity data of the PVA and PVA/(20%)FS composites doped with KOH at various temperatures was calculated using the AC impedance spectra. Fig. 3 shows the Nyquist plots for the PVA membrane and PVA/(20%)FS electrolytes impregnated in 1 M KOH at 60 °C. The full range Nyquist plot is shown in Fig. 3 with the high frequency range data detailed in the insert. The intercept on the real axis represents the bulk resistance, R_b, of the membranes. The R_b value was decreased with increasing FS concentration in the PVA membrane. The conductivity values were calculated from R_b data by normalizing with film thickness

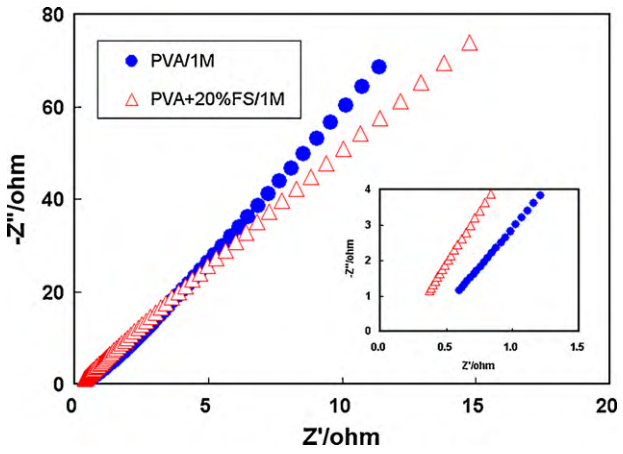

Fig. 3. Nyquist plots of PVA and PVA/(20%)FS electrolytes doped with 1 M KOH at 60 °C. The small insert shows the high frequency range data, which are extracted to obtained resistance and conductivity values.

and electrode contact area. The ionic conductivities of 0.0184 and 0.0583 S cm^{-1} were obtained for PVA/KOH and PVA/(20%)FS/KOH electrolytes, respectively.

The ionic conductivity of the PVA membrane and the PVA/(20%)FS composite doped with 1 and 6 M KOH at different temperatures were measured. The conductivities of both the PVA/KOH and the PVA/FS/KOH electrolytes increased with KOH concentration and FS loading. Typical results are shown in Fig. 4. The maximum conductivity value obtained for the PVA/(20%)FS/KOH electrolyte was 0.16 S cm^{-1} when it was doped in 6 M KOH and operated at 60 °C. The higher concentration of impregnated KOH also resulted in higher conductivity. For instance, the conductivities of the PVA/FS/KOH electrolytes were 0.058, 0.086, and 0.16 S cm^{-1} when doped with 1, 2 [42] and 6 M KOH, respectively. This increase may be ascribed to two reasons. First, a greater percentage of bound water was present in the electrolyte with higher KOH concentration. The bound water does not evaporate at an elevated temperature, and the enhanced water retention improves the wettability of the membrane. Furthermore, the electrolytes immersed in 6 M KOH exhibited higher KOH uptake than those in 1 M KOH. For instance, PVA/FS impregnated in 6 M KOH contained 2.02 g KOH g^{-1} composite, a level that was higher than that in 1 M KOH (with an uptake of 0.96 g KOH g^{-1}). Higher KOH uptake and higher bound-water levels resulted in the higher conductivity for the electrolyte immersed in the higher-concentration KOH solution (6 M).

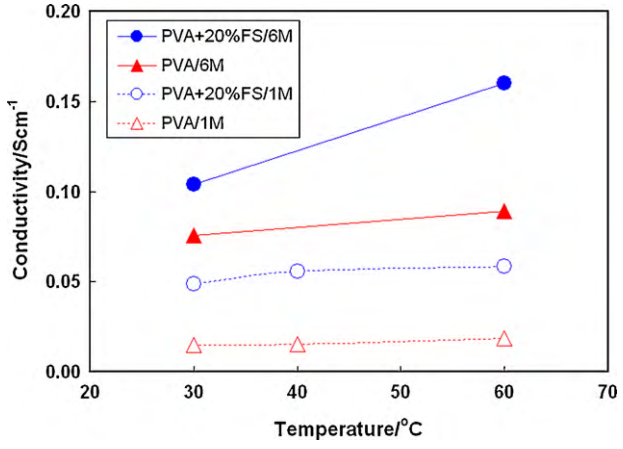

Fig. 4. Ionic conductivities of PVA/KOH and PVA/FS/KOH electrolytes after being immersed in 1 and 6 M KOH at different temperatures.

Additionally, the hydroxide ion may diffuse faster in the FS-containing composite because of a higher free volume in the polymer matrix [36]. During film formation, the steric hindrance of the nanoparticles prevents polymer chain alignment and packing and leads to more amorphous regions and the formation of more free volume in the polymer matrix [36]. This enlarged free volume provides a pathway for the diffusion of the smaller hydroxide ion and water [36]. However, the free volume (with a diameter of 4.46 Å [36]) allows less methanol (with a diameter of 3.63 Å [45]) transport than water (with a diameter of 2.64 Å [45]) permeation, resulting in the suppressed methanol permeability discussed earlier. Therefore, the conductivity was improved, and the methanol cross-over was retarded in the FS-containing composite. As the temperature was raised, the diffusivity was accelerated because of the higher kinetic energy of the hydroxide ions and the expanded free volume in PVA associated with the high temperature. Therefore, the conductivity was increased for the PVA/FS composite polymer membranes at elevated temperatures. For comparison, Yang et al. [12] reported that the ionic conductivities of the alkaline-doped PVA/(20%)HAP (hydroxyapatite) and PVA/(2%)TiO_2 composite were 0.044 and 0.018 S cm^{-1} at 30 °C, respectively, at 30 °C, which were lower than that of our PVA/(20%)FS/KOH electrolyte doped with 2 M KOH (0.076 S cm^{-1} at 30 °C).

3.3. Reproducibility measurement

Reproducibility of open-circuit voltage (V_{oc}) and experimental error in the maximum power density (P_{max}) values for direct methanol alkaline fuel cell performance measurements at 40 °C are shown in Fig. 5(a) and (b). The experimental errors for the open-circuit voltage and maximum power density were 0.021 V and 0.64 mW cm^{-2}, respectively, corresponding to coefficients of variation of 2.19 and 2.23%. The polarization losses in the voltage–current density (*V–I*) curve can be classified into three regions: (i) in the activation energy region, the initial voltage drops quickly at low current density, (ii) in the ohmic region, the linear voltage drop is observed due to ohmic loss, and (iii) in the concentration loss region, the voltage drop is due to reactant deficiency at high current density. The exact mechanism of initial voltage drop is not clearly demonstrated. Hoster et al. [46,47] studied the methanol oxidation on the surface of Pt–Ru model electro-catalysts used for fuel cell electrodes. They attributed that the fast initial voltage drop at low current density is due to the non-equilibrium concentration among the active Ru oxide catalyst. Yu et al. [48] studied performance comparison between the miniature silicon wafer fuel cell with smaller size channels and a standard fuel cell and reported the initial drop of the voltage at very low current density was due to an electrochemical activating process, which was caused by the sluggish kinetics of oxygen reduction at the cathode surface.

3.4. Effect of cathode gas on cell performance

Fig. 6 shows the open-circuit voltage and power density values for the PVA/(20%)/FS/KOH electrolyte using both humidified air and oxygen as the cathode feed. It shows that the cell performance with oxygen was higher than that with air, and this result was probably due to the reduced oxidant activity of air, which leads to activation loss and concentration loss. The open-circuit potential and peak power density of the DMAFC with an oxygen-feed were 1.0 V and 39 mW cm^{-2}, and those with the air-feed were 0.92 V and 32 mW cm^{-2}, respectively. The peak power density using pure oxygen was 22% higher than that with air-feed.

There are limited reports available on the effect of cathode gas identity (oxygen vs. air) on DMAFC performance when using hydroxide-containing electrolytes. Scott et al. [11] reported that DMAFCs with oxygen as the cathode feed performed better than

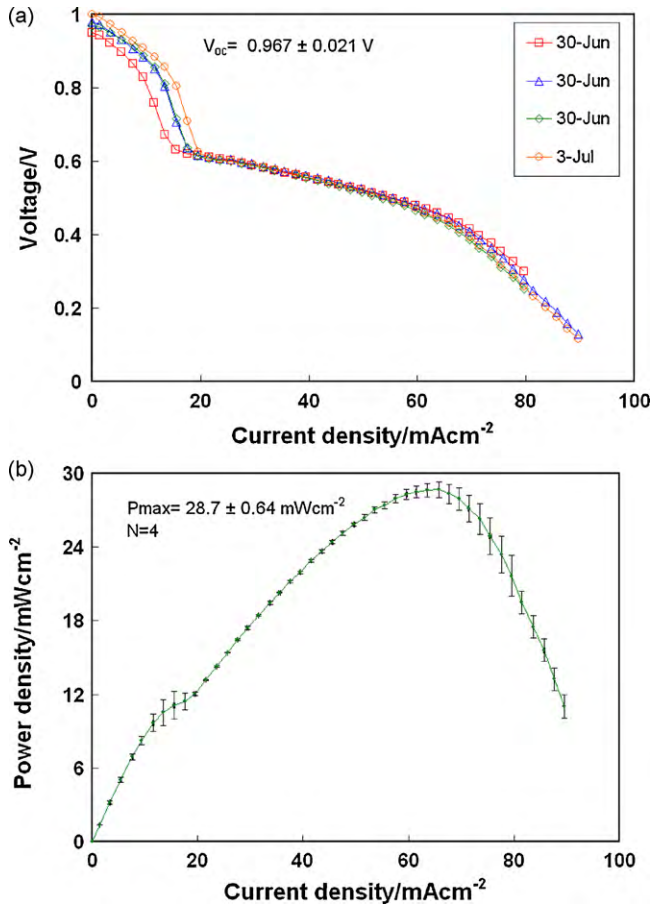

Fig. 5. (a) Reproducibility of open-circuit voltage (V_{oc}) and (b) experimental error in the maximum power density (P_{max}) values for direct methanol alkaline fuel cell performance measurements at 40 °C (anode: 2 M methanol in 6 M KOH with a flow rate of 5 mL min^{-1}, cathode: humidified oxygen with a flow rate of 100 mL min^{-1}).

those using air. The open-circuit potential and peak power density of a DMAFC system using oxygen were around 0.665 V and 10.8 mW cm^{-2}, respectively; and these values were higher than those when using air as cathode feed (0.655 V and 8.4 mW cm^{-2}). For direct methanol fuel cells with proton-exchange membranes, some authors observed that the cell performance was better with oxygen as the cathode feed than with air. Ge and Liu [49] studied the cell performance of a Nafion 117 membrane and found that the

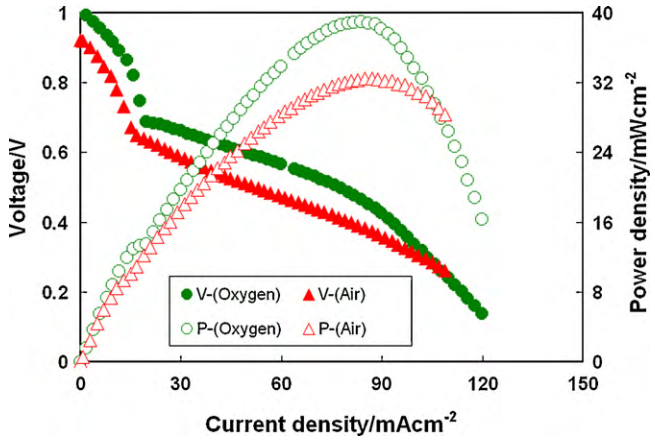

Fig. 6. Effect of cathode feed gas on direct methanol alkaline fuel cell performance at 60 °C (anode: 2 M methanol in 6 M KOH with a flow rate of 5 mL min^{-1}, cathode: humidified oxygen with a flow rate of 100 mL min^{-1}).

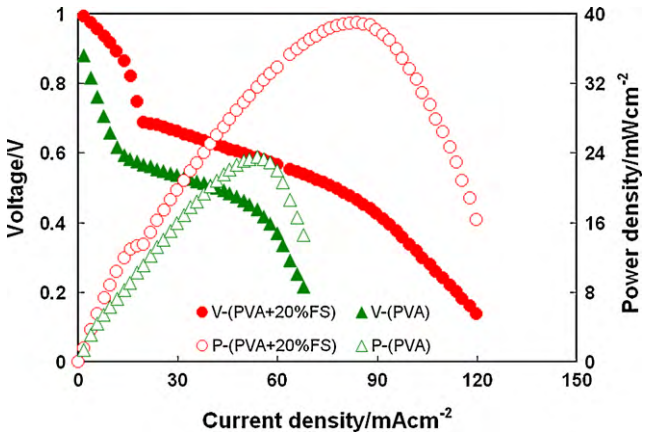

Fig. 7. Effect of fumed silica addition in PVA on DMAFC cell performance at 60 °C (anode: 2 M methanol in 6 M KOH with a flow rate of 5 mL min^{-1}, cathode: humidified oxygen with a flow rate of 100 mL min^{-1}).

DMFC's peak power density with oxygen was about 100% higher than when using air as the cathode feed. Seo and Lee [50] also reported improved results; oxygen as the cathode feed generated 145% higher power than air as the cathode feed. Although the difference in the power densities of our DMAFCs between oxygen- and air-feed was lower than their impacts on the proton-exchange DMFCs, the improved power output when using oxygen as the oxidant was confirmed.

3.5. Effect of fumed silica addition on the cell performance

Fig. 7 shows the polarization curves and the power densities obtained for the single cell using the PVA/KOH and the PVA/(20%)FS/KOH electrolytes and 2 M methanol and 6 M KOH solution as fuel at 60 °C. The PVA/(20%)FS/KOH electrolyte exhibited better cell performance than that of the PVA/KOH electrolyte. There was a 12.5% increase in the open-circuit voltage when the PVA/KOH electrolyte was changed to the PVA/(20%)FS/KOH electrolyte (0.88 and 0.99 V, respectively). Moreover, the peak power density of the DMAFC with the PVA/(20%)FS/KOH electrolyte was 65% higher than that of the PVA/KOH electrolyte (39.0 mW cm^{-2} vs. 23.5 mW cm^{-2}). The higher open-circuit potential indicated that the methanol transport was suppressed when using the FS-containing electrolyte. Limited methanol was transported into the anode, and the methanol oxidation potential on the anode was minimized. The higher power density can also be ascribed to the higher conductivity in the composite polymer electrolyte because of the FS incorporation discussed earlier. As seen from the polarization curves in Fig. 7, the slope of the ohmic loss region when using the PVA/FS/KOH electrolyte was lower than that for the PVA/KOH electrolyte. This difference implies a smaller ohmic loss from the MEA when employing the PVA/FS/KOH electrolyte. The higher ionic conductivity of the PVA/FS/KOH electrolyte contributed to its higher power output than that of the PVA/KOH electrolyte.

Table 1 shows the peak power density results reported by different researchers using methanol and alkali as the anode feed. Verma and Basu [20] obtained a power density of 15 mW cm^{-2} with 2 M methanol and 3 M KOH liquid electrolytes at 65 °C. Other literature reports are for DMAFC with solid electrolytes. Please be aware that the peak power density data were generated at various operating conditions (with some critical parameters shown in Table 1). The results are better compared under similar test conditions. For instance, we can compare results at 60 °C, 1–2 M methanol concentration, and 4–5 mg cm^{-2} catalyst loading. Yang et al. [13,51] obtained peak power densities of 4.13 and 7.54 mW cm^{-1}, respectively, using KOH-doped cross-linked PVA

Table 1
Comparison of peak power densities of DMAFCs presented in the literature (data sorted according to electrolyte phase, temperature, methanol and alkali concentrations).

Electrolyte	Operating conditions			Peak power density (mW cm^{-2})	Source
	Anode catalyst (loading in mg cm^{-2})	Temperature (°C)	Feed methanol + alkali		
Liquid alkali	Pt (1)	65	2 M + 3 M KOH	15	Verma and Basu [20]
KOH-doped PBI	Pt–Ru (2)	90	2 M + 2 M KOH	31	Hou et al. [32]
KOH-doped PVA/FS	Pt–Ru (5)	60	2 M + 6 M KOH	39	This work
KOH-doped PVA/FS	Pt–Ru (5)	60	2 M + 2 M KOH	15.3	Lue et al. [42]
KOH-doped PVA cross-linked with sulfosuccinic acid	Pt–Ru (4.5)	60	2 M + 2 M KOH	4.13	Yang et al. [51]
KOH-doped PVA/TiO_2	Pt–Ru (4)	60	2 M + 2 M KOH	7.54	Yang [13]
KOH-doped PVA/FS	Pt–Ru (5)	60	2 M + 1 M KOH	7.9	Lue et al. [42]
Nafion 117, Na-form	Pt (2)	60	2 M + 1 M NaOH	4.4	Yu et al. [28]
Anion-exchange membrane (ADP, Solvay), OH-form	Pt (2.14)	60	2 M + 1 M NaOH	10.1	Yu and Scott [5]
Anion-exchange membrane (ADP, Solvay), OH-form	Pt (0.526)	60	2 M + 1 M NaOH	17.8	Yu and Scott [31]
KOH-doped PVA/FS	Pt–Ru (5)	60	1 M + 6 M KOH	30	This work
KOH-doped PVA/FS	Pt–Ru (5)	60	1 M + 1 M KOH	10.2	Lue et al. [42]
Anion-exchange membrane (ADP, Solvay), OH-form	Pt (1)	60	1 M methanol	8.5	Scott et al. [11]
poly(ethylene-*co*-tetrafluoroethylene) based anion-exchange membrane	Pt–Ru (4)	50	2 M methanol	2.1	Varcoe et al. [29]
Anion-exchange membrane (AHA, Tokuyama), OH-form	Pt–Ru (4)	50	1 M + 1 M KOH	6.1	Matsuoka et al. [30]
KOH-doped PVA/FS	Pt–Ru (5)	40	2 M + 6 M KOH	30	This work
KOH-doped PVA/FS	Pt–Ru (5)	30	2 M + 6 M KOH	15	This work
KOH-doped PVA/HAP	Pt–Ru (4)	25	2 M + 8 M KOH	11.48	Yang et al. [34]
KOH-doped PVA/TiO_2	Pt–Ru (3.6)	25	2 M + 4 M KOH	9.25	Yang et al. [33]
Anion-exchange membrane (AHA, Tokuyama), OH-form	Pt (1.8)	25	2 M + 3 M KOH	11.5	Kim et al. [26]
Anion-exchange membrane (ADP, Solvay), OH-form	Pt (2)	20	2 M + 4 M KOH	18	Coutanceau et al. [27]

and PVA/TiO_2 electrolytes at 60 °C using 2 M methanol and 2 M KOH as the anode feed. Matsuoka et al. [30] obtained a peak power density of 6.1 mW cm^{-1} at 50 °C with hydrocarbon-based anion-exchange membrane using 1 M methanol and 1 M KOH as the anode feed. Varcoe et al. [29] prepared MEA using poly(ethylene-*co*-tetrafluoroethylene) derived anion-exchange membrane and attained peak power density of 2.1 mW cm^{-2} using 2 M methanol fuel. The electrochemical results in this study are superior to these literature data.

Other studies demonstrated the feasibility of extending beyond the normal operating conditions and reported DMAFC performance data. Yu and Scott [31] achieved a peak power density of 17.8 mW cm^{-2} at 0.526 mg cm^{-2} Pt loading using Morgane-ADP® anion-exchange membrane and 60 °C. Hou et al. [32] obtained a high peak power density of 31 mW cm^{-1} at 90 °C with alkali-doped polybenzimidazole electrolyte. Coutanceau et al. [27] reported 18 mW cm^{-1} at 20 °C with ADP anion-exchange membrane. These references also serve bench marks for future development.

The PVA/FS/KOH electrolyte for DMAFCs showed a much higher power density (39.0 mW cm^{-2} at 60 °C) than those reported in previous research (Table 1). The FS plays an important role in reducing the methanol permeability (Fig. 2), in increasing the thermal and mechanical strength of the FS-incorporated PVA membranes [35], and in enhancing the electrolyte conductivity (Fig. 4). The conductivity of the PVA/FS/KOH electrolyte was almost one order of magnitude higher than the other hydroxide-exchange membranes [13,32,34]. These benefits resulted in a high open-circuit voltage and high power density for the DMAFCs.

3.6. Effect of methanol concentration on the cell performance

Fig. 8 shows the cell polarization curves and the power density data of the DMAFCs with the PVA/FS/KOH electrolytes in different methanol concentrations in 6 M KOH for the anode feed at 60 °C. As the methanol concentration increased from 1 to 2 M, the open-circuit voltage and the peak power density increased. The open-circuit potential and peak power density for 2 M methanol were 1.0 V and 39 mW cm^{-2}, which were higher than the open-circuit potential and the peak power density for 1 M methanol (0.98 V and 30 mW cm^{-2}) at 60 °C. This trend was in agreement with the literature results. When the concentration of methanol was increased to 2 M, Yu and Scott [11,31] also observed the increase in cell performance of a DMAFC that used a perfluorocarbon anion-exchange membrane. They reported a maximum power density of 17.8 mW cm^{-2} at 60 °C with 2 M methanol + 1 M NaOH when employing their synthesized anode and cathode catalysts. They also observed a decrease in the power density as the methanol concen-

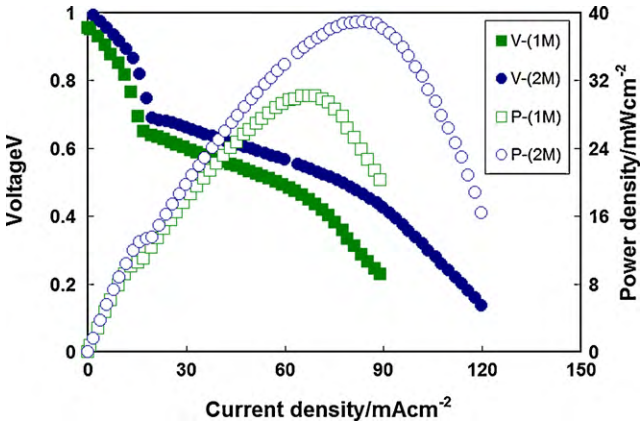

Fig. 8. Effect of methanol concentration on DMAFC performance with PVA/(20%)FS/KOH electrolyte at 60 °C (anode: methanol in 6 M KOH with a flow rate of 5 mL min^{-1}, cathode: humidified oxygen with a flow rate of 50 mL min^{-1} for 1 M methanol or 100 mL min^{-1} for 2 M methanol).

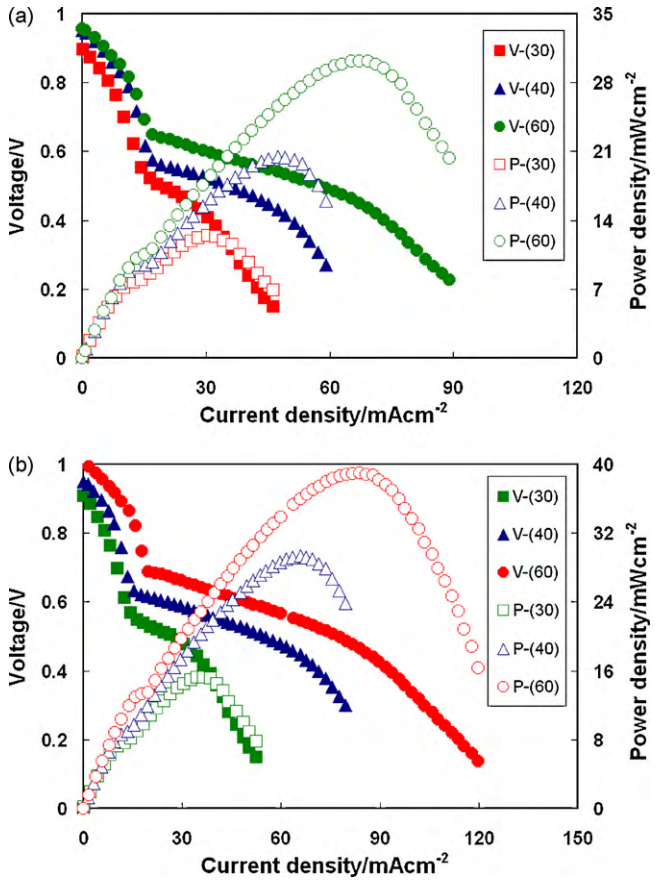

Fig. 9. Effect of temperature on the cell performance of DMAFCs with PVA/(20%)FS/KOH electrolyte and using (a) 1 M and (b) 2 M methanol in 6 M KOH (anode: methanol in 6 M KOH with a flow rate of 5 mL min^{-1}, cathode: humidified oxygen with a flow rate of 50 mL min^{-1} for 1 M methanol or 100 mL min^{-1} for 2 M methanol).

tration was raised to 4 M [5,11]. The higher methanol concentration increases the oxidation rate at the anode and generates more electrons through the external circuit. With an even higher methanol concentration, excess un-reacted methanol may cross-over to the anode and produce an unwanted oxidation reaction that lowers the effective cell potential. Therefore, excess methanol does not benefit DMAFC function.

3.7. Effect of temperature on the cell performance

Fig. 9(a) shows the cell polarization curves and the power density values for the DMAFC containing the PVA/(20%)FS/KOH electrolyte fed with 1 M methanol and 6 M KOH fuel at 30–60 °C. The cell potential and the power density increase with increasing the operation temperature because of the faster catalytic kinetics achieved at higher temperatures. The peak power density of 30 mW cm^{-2} was obtained at a potential of 0.47 V with a current density of 66 mA cm^{-2} at 60 °C, and the peak power density of the DMAFC was decreased to 20 and 12 mW cm^{-2} for 40 and 30 °C, respectively. Fig. 9(b) shows the dependence of cell performance on temperature when using 2 M methanol in 6 M KOH fuel at 30–60 °C. The peak power density of 39 mW cm^{-2} was obtained at a potential of 0.47 V with a current density of 84 mA cm^{-2} at 60 °C, and the peak power density of the DMAFC was decreased to 30 and 15 mW cm^{-2} for 40 and 30 °C, respectively.

Yu et al. [52] reported that the oxidation of 2 M methanol in 0.5 M NaOH solution is 109 and 114 mV dec^{-1} at 20 and 60 °C, and they confirmed the higher methanol oxidation achieved at a higher

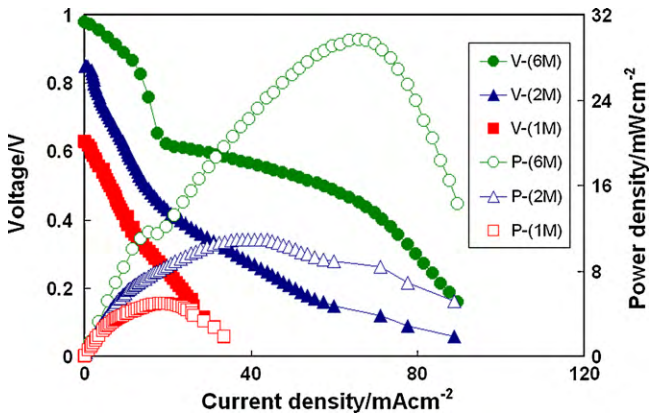

Fig. 10. Dependency of DMAFC performance on KOH concentration at 40 °C (PVA/(20%)FS/KOH electrolyte (anode: 2 M methanol in KOH with a flow rate of 5 mL min^{-1}, cathode: humidified oxygen with a flow rate of 100 mL min^{-1}).

temperature. Scott et al. [11] and Yang [13] also observed that the peak power density of the DMAFC increases as the operation temperature increases from 25 to 60 °C. High temperatures accelerate methanol oxidation reactions [52,53]. Therefore, more electrons were produced at a high temperature, thereby increasing the current density. Meanwhile, higher temperature enhanced the ionic conductivity of the electrolyte (Fig. 4) and of the MEA (shown in the lower slope of the ohmic loss regions in Fig. 9), slowed the voltage loss, and maintained high power output. The overall fuel cell performance was greatly enhanced at an elevated temperature.

3.8. Effect of KOH concentration on the cell performance

Fig. 10 shows the cell polarization curves and the power density results of the DMAFC fed with 1–6 M KOH and 2 M methanol while using the PVA/(20%)FS/KOH electrolyte at 40 °C. The data shows that the cell performance increased with increasing the concentration of KOH. The polarization curve showed an open-circuit potential of 0.62 and 1.0 V for 1 and 6 M KOH, respectively. The higher KOH concentration supplied more OH^- ions that are needed for the oxidation half-reaction on the anode (Fig. 1(a)). The peak power density with 6 M KOH was 30 mW cm^{-2} at 40 °C, which was significantly higher than the values of 5 and 11 mW cm^{-2} achieved using the DMAFC with 1 and 2 M KOH, respectively. Yang [13] showed 7.54 mW cm^{-1} peak power density using 2 M methanol and 2 M KOH as anode feed with KOH-doped PVA/TiO_2 electrolyte at 60 °C. As the KOH concentration was increased to 4 M, a peak power density of 9.25 mW cm^{-1} was achieved at room temperature [33]. Our data and Yang's results confirm the significant enhancement on cell performance by increasing the KOH concentration.

The slopes of the ohmic regions in Fig. 10 were used to calculate the resistances of the MEAs. The electrolyte resistance was obtained from AC impedance measurement (shown in Section 2.4). Table 2 shows the ohmic resistance values of the MEAs using PVA/FS/KOH and of the corresponding electrolytes at 40 °C with 1–6 M KOH. The resistance of both the MEA and electrolyte decreased with increases in KOH concentration. The MEA resistance was higher than the electrolyte resistance because the former represented the overall resistance contributed from the electrolyte, the gas diffusion electrode, the interface(s), the graphite flow-field plates, and the current collector. The resistance difference (shown in the last column of Table 2) between the MEA and the electrolyte was ascribed to the gas diffusion electrode, the interface(s), the graphite flow-field plates, and the current collector. The higher KOH concentration not only reduced the electrolyte resistance, but it also suppressed the other resistances from the non-electrolyte compo-

Table 2
Resistance of the membrane electrode assembly (MEA)[a] and the electrolyte alone while using different concentrations of KOH.

KOH concentration	Resistance (MEA) (Ω)	Resistance (electrolyte) (Ω)	Resistance (other)[b] (Ω)
1 M	2.77	0.25	2.52
2 M	1.40	0.18	1.22
6 M	0.77	0.14	0.63

[a] Electrolyte: KOH-doped PVA/(20%)FS, 40 °C.
[b] Resistance contributed from gas diffusion electrode, the interface(s), the graphite flow-field plates, and the current collector. The value was estimated by subtracting the "resistance (electrolyte)" values (data from Fig. 4 and [42]) from the "resistance (MEA)" values (data from *V–I* curves in Fig. 10).

nents. The cell performance was significantly improved by adding high-concentration KOH.

3.9. Durability test

Fig. 11 shows the cell performance during a long-term stability test for the DMAFCs at a constant current of 20 mA cm^{-2} at 40 °C. The data were recorded over a continuous operating period of 100 h with 30-min off-periods every 20 h. During the stability test, the cell potential of 0.56 V for the DMAFC was quite stable and corresponds to the cell potential at a constant current of 20 mA cm^{-2} at 40 °C (Fig. 9(a)). During the off-period, the cell potential immediately returned to 0.94 V, which matched the open-circuit potential at 40 °C (Fig. 9(a)). Yang [13] reported the results of a long-term stability test for DMAFCs using a PVA/TiO_2/KOH electrolyte at 25 °C. In that test, the cell potential was 0.17 V at 20 mA cm^{-2} and returned to 0.77 V (the open-circuit potential) during the off-period. Our long-term stability results had a trend similar to that of Yang's observation but with a higher cell potential and an increased open-circuit voltage for the DMAFCs in this work. In this operation mode, the methanol/KOH discharge was recycled into the feed reservoir to save the fuel and to avoid refill interruptions. The produced carbon dioxide from the methanol oxidation reaction may have been retained in this recycle stream. During the 100-h period of operation, the accumulated carbon dioxide was not significant enough (less than 0.1 mol; (20 mA cm^{-2})(5 cm^2)(100 h)(3600 s/1 h)(1 mol e$^-$/96,500 C)(1 mol CO_2/6 mol e$^-$) = 0.062 mol) to result in any detrimental effects on the cell potential or on the power density. Furthermore, the weak carbonate has little impact on the pH value of the fuel and on the

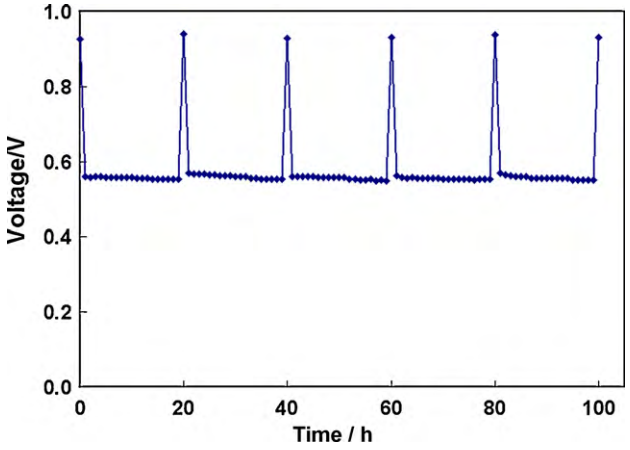

Fig. 11. Long-term performance of the DMAFC with the PVA/(20%)FS/KOH electrolyte in 1 M methanol and 6 M KOH fuel at 40 °C (operated at a constant current of 20 mA cm^{-2} with a 30-min off-period every 20 h, anode: 1 M methanol in 6 M KOH with a flow rate of 5 mL min^{-1}, cathode: humidified oxygen with a flow rate of 50 mL min^{-1}).

electrolyte conductivity. Padhy and Reddy [54] studied the DMFC performance of recycled methanol solution up to 100 h using Nafion 117 as the electrolyte and 2 M methanol feed at 70 °C, and found ~3% efficiency drop compared with non-recycled fuel. Our result and Padhy and Reddy's data demonstrate that the recycled methanol fuel do not sacrifice the cell performance at this time span.

4. Conclusion

The solid electrolyte consisting of alkaline-doped PVA/FS composites was successfully prepared by a solution-casting method. Ionic conductivities and suppressed methanol cross-over rates were improved by adding the FS nanoparticles. The temperature and concentrations of methanol and KOH solutions were key operating parameters influencing the performance of the DMAFCs. An optimal open-circuit potential and a peak power density of 1.0 V and 39 mW cm^{-2} were obtained using a 2 M methanol fuel in 6 M KOH at 60 °C with the PVA/(20%)FS/KOH electrolyte. These electrochemical results were superior to those reported at similar operating conditions in the literature. Long-term cell performance was sustained during a 100-h continuous operation. Overall, the PVA/FS/KOH electrolyte is an inexpensive material and can be used for direct methanol alkaline fuel cells.

Acknowledgement

We thank the National Science Council of Taiwan for financial support (NSC 97-2221-E-182-029).

References

[1] N. Nakagawa, Y. Xiu, J. Power Sources 118 (2003) 248–255.
[2] A.S. Aricò, S. Srinivasan, V. Antonucci, Fuel Cells 1 (2001) 133–161.
[3] C.Y. Chen, P. Yang, J. Power Sources 123 (2003) 37–42.
[4] K. Dyer, J. Power Sources 106 (2002) 31–34.
[5] E.H. Yu, K. Scott, J. Power Sources 137 (2004) 248–256.
[6] P. Costamagna, S. Srinivasan, J. Power Sources 102 (2001) 242–252.
[7] M.A. Hickner, H. Ghassemi, Y.S. Kim, B.R. Einsla, J.E. McGrath, Chem. Rev. 104 (2004) 4587–4612.
[8] B.R. Einsla, Y.S. Kim, M.A. Hickner, Y.T. Hong, M.L. Hill, B.S. Pivovar, J.E. McGrath, J. Membr. Sci. 255 (2005) 141–148.
[9] Q. Li, R. He, J.O. Jensen, N.J. Bjerrum, Chem. Mater. 15 (2003) 4896–4915.
[10] A. Huang, C. Xia, C. Xiao, L. Zhuang, J. Appl. Polym. Sci. 100 (2006) 2248–2251.
[11] K. Scott, E.H. Yu, G. Vlachogiannopoulosa, M. Shivare, N. Duteanu, J. Power Sources 175 (2008) 452–457.
[12] C.-C. Yang, C.-T. Lin, S. Chiu, Desalination 233 (2008) 137–146.
[13] C.-C. Yang, J. Membr. Sci. 288 (2007) 51–60.
[14] C. Sollogoub, A. Guinault, C. Bonnebat, M. Bennjima, L. Akrour, J.F. Fauvarque, L. Ogier, J. Membr. Sci. 335 (2009) 37–42.
[15] M.A. Al-Saleh, S. Gültekin, A.S. Al-Zakri, H. Celiker, J. Appl. Electrochem. 24 (1994) 575–580.
[16] Y. Wang, L. Li, L. Hu, L. Zhuang, J.T. Lu, B.Q. Xu, Electrochem. Commun. 5 (2003) 662–666.
[17] A.V. Tripkovic, K.D. Popovic, B.N. Grgur, B. Blizanac, P.N. Ross, N.M. Markovic, Electrochim. Acta 47 (2002) 3707–3714.
[18] A.V. Tripkovic, K.D. Popovic, J.D. Lovic, V.M. Jovanovic, A. Kowal, J. Electroanal. Chem. 572 (2004) 119–128.
[19] J. Prabhuram, R. Manoharan, J. Power Sources 74 (1998) 54–61.
[20] A. Verma, S. Basu, J. Power Sources 145 (2005) 282–285.
[21] M. Cifrain, K.V. Kordesch, J. Power Sources 127 (2004) 234–242.
[22] G.F. McLean, T. Niet, S. Prince-Richard, N. Djilali, Int. J. Hydrogen Energy 27 (2002) 507–526.
[23] L. Li, Y.X. Wang, J. Membr. Sci. 262 (2005) 1–4.
[24] J. Fang, P.K. Shen, J. Membr. Sci. 285 (2006) 317–322.
[25] J.R. Varcoe, R.C.T. Slade, Electrochem. Commun. 8 (2006) 839–843.
[26] J. Kim, T. Momma, T. Osaka, J. Power Sources 189 (2009) 999–1002.
[27] C. Coutanceau, L. Demarconnay, C. Lamy, J.-M. Leger, J. Power Sources 156 (2006) 14–19.
[28] E.H. Yu, K. Scott, R.W. Reeve, J. Appl. Electrochem. 36 (2006) 25–32.
[29] J.R. Varcoe, R.C.T. Slade, E.L.H. Yee, S.D. Poynton, D.J. Driscoll, D.C. Apperley, Chem. Mater. 19 (2007) 2686–2693.
[30] K. Matsuoka, Y. Iriyama, T. Abe, M. Matsuoka, Z. Ogumi, J. Power Sources 150 (2005) 27–31.
[31] E.H. Yu, K. Scott, J. Appl. Electrochem. 35 (2005) 91–96.

[32] H. Hou, G. Sun, R. He, B. Sun, W. Jin, H. Liu, Q. Xin, Int. J. Hydrogen Energy 33 (2008) 7172–7176.
[33] C.C. Yang, S.J. Chiu, K.T. Lee, W.C. Chien, C.T. Lin, C.A. Huang, J. Power Sources 184 (2008) 44–51.
[34] C.C. Yang, S.J. Chiu, C.T. Lin, J. Power Sources 177 (2008) 40–49.
[35] S.J. Lue, J.-Y. Chen, J.M. Yang, J. Macromol. Sci. Phys. 47 (2008) 39–51.
[36] S.J. Lue, D.-T. Lee, J.-Y. Chen, C.-H. Chiu, C.-C. Hu, Y.C. Jean, J.-Y. Lai, J. Membr. Sci. 325 (2008) 831–839.
[37] S.J. Lue, S.-J. Shieh, Polymer 50 (2009) 654–661.
[38] S.J. Lue, Te-S. Shih, Ta-C. Wei, Korean J. Chem. Eng. 23 (2006) 441–446.
[39] H.-S. Kim, J.-H. Shin, S.-I. Moon, M.-S. Yun, Electrochemical properties of poly(tetra ethylene glycol diacrylate)-based gel electrolytes for lithium-ion polymer batteries, J. Power Sources 119–121 (2003) 482–486.
[40] J.-U. Kim, C.-H. Sung, S.-I. Moon, H.-B. Gu, Proceedings of the 5th International Conference on Properties and Applications of Dielectric Materials, May 25–30, 1997, Seoul, Korea, 1997.
[41] Y. Gao, G.P. Robertson, M.D. Guiver, X. Jian, J. Polym. Sci. Part A: Polym. Chem. 41 (2003) 497–507.
[42] S. J. Lue, K.P.O. Mahesh, W.T. Wang, C.C. Yang, J. Membr. Sci., submitted for publication.
[43] X. Liu, Y. Sun, X. Deng, J. Membr. Sci. 325 (2008) 192–198.
[44] C.-C. Yang, Y.-J. Lee, J.M. Yang, J. Power Sources 188 (2009) 30–37.
[45] R.C. Reid, J.M. Prausmitz, B.E. Poling, The Properties of Gases and Liquids, McGraw Hill Book Co., Singapore, 1987.
[46] H. Hoster, T. Iwasita, H. Baumgartner, W. Vielstich, Phys. Chem. Chem. Phys. 3 (2001) 337–346.
[47] H. Hoster, T. Iwasita, H. Baumgartner, W. Vielstich, J. Electrochem. Soc. 148 (2001) A496–A501.
[48] J. Yu, P. Cheng, Z. Ma, B. Yi, J. Power Sources 124 (2003) 40–46.
[49] J. Ge, H. Liu, J. Power Sources 142 (2005) 56–69.
[50] S.H. Seo, C.S. Lee, Energy Fuels 22 (2008) 1212–1219.
[51] C.-C. Yang, S.-J. Chiu, W.-C. Chien, J. Power Sources 162 (2006) 21–29.
[52] E.H. Yu, K. Scott, R.W. Reeve, J. Electroanal. Chem. 547 (2003) 17–24.
[53] M. Uma, R. Manoharan, Bull. Electrochem. 12 (1996) 196–200.
[54] B.R. Padhy, R.G. Reddy, J. Power Sources 153 (2006) 125–129.